Photoluminescence mechanism model for oxidized porous silicon and nanoscale-silicon-particle-embedded silicon oxide

G. G. Qin[1,2] and Y. J. Li[1]
[1]*Department of Physics and State Key Lab for Mesoscopic Physics, Peking University, Beijing 100871, China*
[2]*International Center for Materials Physics, Academia Sinica, Shenyang 110015, China*
(Received 23 November 2002; published 13 August 2003)

There is much debate about the photoluminescence (PL) mechanisms of the nanoscale Si/Si oxide systems containing oxidized porous silicon and a nanoscale-Si-particle (NSP)—embedded Si oxide deposited by chemical vapor deposition, sputtering, or Si-ion implanting into Si oxide. In this paper, we suggest that two competitive processes, namely, the quantum confinement (QC) process and the quantum confinement-luminescence center (QCLC) process, take place in the PL. The photoexcitation occurs in the NSPs for both of the processes, while the photoemission occurs either in the NSPs for the QC process or in the luminescence centers (LCs) in Si oxide adjacent to the NSPs for the QCLC process. The rates of the two processes are compared quantitatively. Which process plays the major role in PL is determined by the capture cross section, the luminescence efficiency, and the density of the LCs, and the sizes of the NSPs. For a nanoscale Si/Si oxide system with the LCs having certain capture cross-section and luminescence efficiency, the higher the LC density and the larger the sizes of NSPs, the more beneficial for the QCLC process to surpass the QC process, and vice versa. For certain LC parameters, there is a critical most probable size for the NSPs. When the most probable size of the NSPs is larger than the critical one, the QCLC process dominates the PL, and when the most probable size of the NSPs is smaller than the critical one, the QC process dominates the PL. When the most probable size of the NSPs is close to the critical one, both the QC and QCLC processes should be taken into account. We have used this model to discuss PL experimental results reported for some nanoscale Si/Si oxide systems.

DOI: 10.1103/PhysRevB.68.085309 PACS number(s): 78.55.−m, 78.67.−n

INTRODUCTION

In 1990 Canham reported strong visible photoluminescence (PL) from porous Si at room temperature,[1] and Tagaki *et al.* observed room-temperature visible PL from a nanoscale-Si-particle (NSP)-embedded Si oxide produced by microwave plasma decomposition of SiH_4 and H_2 or SiH_4, H_2 and an Ar gas mixture.[2] In both papers they used the quantum confinement (QC) model to explain the PL. It was considered that the photoemission occurs inside the NSPs with energy gaps larger than that of the bulk Si due to the QC effect. In fact, in many cases the PL experimental results for porous Si and the NSP-embedded Si oxide are so complicated that the QC model seems difficult to explain these results. In fact, there is a long debate concerning the PL mechanisms of porous Si and the NSP-embedded Si oxide, and for porous Si at least 24 models different from the QC model were suggested in 1992–1997.[3] When a porous Si sample is prepared by anodization and lays in the air, it will be oxidized quickly. It was reported that after 30-min air exposure about 1–2 % oxygen atoms presented in the porous Si layers.[4] Therefore, most porous Si studied is oxidized porous Si. Considering that the NSPs in both oxidized porous Si and the NSP-embedded Si oxide are covered by Si oxide, in this paper we refer to both of them as nanoscale Si/Si oxide systems. For PL from these systems, Qin and Jia suggested a common mechanism model, the so-called quantum confinement–luminescence center (QCLC) model, which claimed that the photoexcitation of electron-hole pairs occurs mainly in the NSPs, while most of the photoexcited electrons and holes tunnel into the luminescence centers (LCs) in the surrounding Si oxide layers and radiatively recombine there.[5] Recently, some authors suggested that more than one type of mechanism were needed in interpreting PL from the nanoscale Si/Si oxide systems. For example, it was suggested that for the *S* (slow)-band luminescence the QC model works, but the *F* (fast)-band luminescence is very likely to originate from contaminated or defective Si oxides.[6] Based on the experiment results reported in Refs. 7 and 8, we suggested that there are three types of photoexcitation-photoemission processes for electron-hole pairs in the PL from a nanoscale Si/Si oxide system[9]: (A) Both photoexcitation and photoemission occur in the NSPs, as described in the QC model. (B) Photoexcitation occurs in the NSPs and photoemission occurs in LCs in Si oxide adjacent to the NSPs, as described in the QCLC model. (C) Both photoemission and photoexcitation occur in LCs in the Si oxide. A lot of PL experiments for nanoscale Si/Si oxide systems can be qualitatively explained by this physics model. In Ref. 10 it was claimed that for NSPs with larger sizes, the QC model works, but for NSPs with smaller sizes, Si═O bond plays the key role in light emission. In this paper, we consider that in strong-light-emission nanoscale Si/Si oxide systems where the NSPs have high densities, the process (C) can be neglected, and we compare the rates of the processes (A) and (B) quantitatively. The key factors in determining whether process (A) or (B) is the major one in the PL are discussed. For a nanoscale Si/Si oxide system with certain LCs in the Si oxide adjacent to the NSPs, we proved that if NSPs have a large enough average size, the QCLC model works, but if NSPs have a small enough average size, the QC model works. This conclusion seems contrary to that of Ref. 10.

 ©2003 The American Physical Society

THEORY

Two types of photoexcitation-photoemission processes, (A) and (B) in the PL from a strong-light-emission nanoscale Si/Si oxide system as described in the introduction are taken into consideration. The photoemission rates of photons in processes (A) and (B) in the unit volume of the system are referred to as P_{ar} and P_{br}, respectively. We have $P_{ar}=N_{eh}/\tau_{ar}$ and $P_{br}=N_{eh}/\tau_{br}$, where N_{eh} is the density of nonequilibrium electron-hole pairs in NSPs, and τ_{ar} and τ_{br} are radiative recombination lifetimes of the nonequilibrium electron-hole pairs in the processes A and B, respectively. Suppose that all NSPs in the Si oxide/nanoscale Si system are cubes with the same size and using the effective mass and infinitely deep well approximations, Hybertsen obtained[11]:

$$\frac{1}{\tau_{ar}}=a_r\frac{E_0(L)\sin^2(k_0L/2)}{[k_0^2-(2\pi/L)^2]^2L^6}, \tag{1}$$

where

$$a_r=\frac{512\pi^4e^2n_r(|P_{cv}|^2/2m)}{3m\hbar^2c^3k_0^2},$$

$$E_0(L)=E_g+\frac{\hbar^2}{2}\left(\frac{1}{m_l}+\frac{2}{m_t}+\frac{3}{m_h}\right)\left(\frac{\pi}{L}\right)^2,$$

L is the side length of the cubic NSP, n_r the refraction index of Si, P_{cv} is the dipole matrix element for vertical transitions in bulk Si, $k_o=0.85(2\pi/a)$, (a is the lattice constant of Si), m is the mass of an electron in vacuum, m_l and m_t are the longitudinal and transverse effective mass for electrons in Si, respectively, m_h is the effective mass for holes in Si, E_g is the forbidden gap for bulk Si, $\hbar$ is the Planck constant, e is the charge of proton, and c is the speed of light. For a NSP embedded in SiO_2, the potential-well depths for electrons and holes are 3.2 and 4.6 eV, respectively, which are so deep that the infinitely deep well approximation can be used.

In order to calculate $1/\tau_{br}$, the x, y, and z axes are located along the three sides of a cubic NSP. When we consider the tunneling of electrons and holes along, for example, the z direction, the barriers of SiO_2 are considered infinitely deep along the x and y directions, while of the actual depth along the z direction. Therefore, electrons and holes photoexcited in the NSP can only tunnel through the barriers along z direction.[12,13] Figure 1 shows the z-direction electron potential with a SiO_2 layer of thickness d surrounding a NSP and a LC located in the SiO_2 layer. It is supposed that the LC has a negative δ potential. The potential of the LC is $-U_1$ in the range $z=\xi-\varepsilon$ and $\xi+\varepsilon$, and zero outside the range, and when U_1 and ε tend respectively to infinity and zero simultaneously, $2\varepsilon U_1$ remains a constant. U_{oe} is the height of the barrier of Si oxide for electrons. The rate for a carrier (an electron or a hole) in a NSP to hit the SiO_2 barrier at $+z$ (or $-z$) direction is $P_z/2m_zL$, where P_z and m_z are the carrier momentum and effective mass in z direction, respectively. Suppose further that after the photoexcitation the carriers in the NSP relax to the ground states before tunneling. As soon as an electron entering the excited electron state of a LC, the

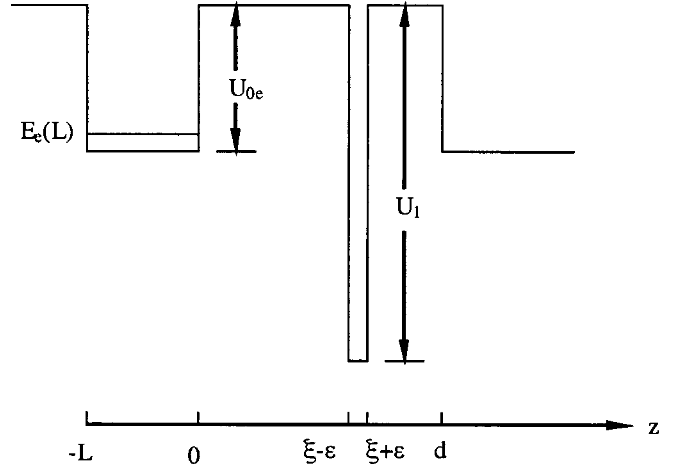

FIG. 1. The z-direction electron potential of a SiO_2 layer of thickness d adjacent to a NSP with width of L and of a LC located in the SiO_2 layer.

lattice will relax to the thermal equilibrium configuration for the excited electron state by emitting multiple phonons. Since the rate for the lattice relaxation [with a time constant of 10^{-10}–10^{-11} sec (Ref. 14)] is usually far faster than the rate for the electron transition from the excited state to the ground state in a LC [the corresponding time constant is $\gtrsim 10^{-8}$ sec (Ref. 6)] to emit a photon. The capture cross section is mainly determined by the rate of the photon emission process, and is approximately independent of the initial energy of the electron in the NSP. Moreover, it is supposed that the LCs distribute uniformly in the SiO_2 layer. The capture cross sections depend on the charged states of the LCs. Assume that the LCs are neutral before illumination, both an electron and a hole can be captured by a neutral LC with capture cross-sections σ_e^o and σ_h^o, then the LC changes to be negative and positive, respectively. Then, a hole and an electron can be captured by the negative and positive LCs, respectively, with very large capture cross-sections. The electron-hole pair in the LC can recombine radiatively or nonradiatively. We have

$$\frac{1}{\tau_{br}}=(V_e\sigma_e^o+V_h\sigma_h^o)N_{\mathrm{LC}}\eta_{\mathrm{LC}}, \tag{2}$$

where

$$V_e=\frac{\pi^3\hbar^3}{4U_{0e}L^4}\left(\frac{1}{m_l}+\frac{2}{m_t}\right)\left[\frac{1}{m_lK_{el}}[1-\exp(-2K_{el}d)]+\frac{2}{m_tK_{et}}[1-\exp(-2K_{et}d)]\right],$$

$$V_h=\frac{9\pi^3\hbar^3}{4U_{0h}L^4m_h^2K_h}[1-\exp(-2K_hd)],$$

$$K_{el}=\frac{\sqrt{2m_l(U_{0e}-E_e(L))}}{\hbar},$$

$$K_{et}=\frac{\sqrt{2m_t[U_{0e}-E_e(L)]}}{\hbar},$$

$$K_h=\frac{\sqrt{2m_h[U_{0h}-E_h(L)]}}{\hbar},$$

$$E_e(L)=\frac{\pi^2\hbar^2}{2L^2}\left(\frac{1}{m_l}+\frac{2}{m_t}\right),$$

$$E_h(L)=\frac{3\pi^2\hbar^2}{2m_hL^2}.$$

In Eq. (2), $N_{\rm LC}$ is the density of the LCs in the SiO_2 layer, $\eta_{\rm LC}$ the luminescence efficiency of the LC, U_{oh} the height of the barrier of SiO_2 for holes, d the thickness of the SiO_2 layer, and $E_e(L)$ and $E_h(L)$ the energies of an electron and a hole in a NSP in their ground states respectively. Because the thickness of the SiO_2 layer is usually larger than 0.4 nm, the factors $\exp(-2K_{el}d)$, $\exp(-2K_{et}d)$, and $\exp(-2K_hd)$ are much smaller than 1 and can be neglected. Then we have

$$V_e=\frac{\pi^3\hbar^4}{4\sqrt{2}}\left(\frac{1}{m_l}+\frac{2}{m_t}\right)\left(\frac{1}{m_l^{3/2}}+\frac{2}{m_t^{3/2}}\right)\frac{1}{U_{oe}[U_{oe}-E_e(L)]^{1/2}L^4},$$
$$V_h=\frac{9\pi^3\hbar^4}{4\sqrt{2}}\left(\frac{1}{m_h^{5/2}}\right)\frac{1}{U_{oh}[U_{oh}-E_h(L)]^{1/2}L^4} \tag{3}$$

V_e in Eq. (3) is not different much from V_h in value. If $\sigma_e^o \gg \sigma_h^o$, we have

$$\frac{1}{\tau_{br}}=b_{re}\frac{N_{\rm LC}\eta_{\rm LC}\sigma_e^o}{[U_{oe}-E_e(L)]^{1/2}L^4}, \tag{4}$$

where

$$b_{re}=\frac{\pi^3\hbar^4}{4\sqrt{2}}\left(\frac{1}{m_l}+\frac{2}{m_t}\right)\left(\frac{1}{m_l^{3/2}}+\frac{2}{m_t^{3/2}}\right)\frac{1}{U_{oe}}$$

is a constant independent of the size of the NSPs and the parameters of the LCs. If $\sigma_h^o\gg\sigma_e^o$, we have

$$\frac{1}{\tau_{br}}=b_{rh}\frac{N_{\rm LC}\eta_{\rm LC}\sigma_h^o}{[U_{oh}-E_h(L)]^{1/2}L^4},$$
$$b_{rh}=\frac{9\pi^3\hbar^4}{4\sqrt{2}}\left(\frac{1}{m_h^{5/2}}\right)\frac{1}{U_{0h}}. \tag{5}$$

Assuming that the LCs are negatively charged before illumination, the hole can be captured by the negatively charged LC with a very large capture cross section σ_h^-, then the LC changes to be neutral, and an electron can be captured by the neutral LC with a medium capture cross-section σ_e^o. We have

$$\frac{1}{\tau_{br}}=\frac{V_e\sigma_e^oV_h\sigma_h^-}{V_e\sigma_e^o+V_h\sigma_h^-}N_{\rm LC}\eta_{\rm LC}\approx V_e\sigma_e^oN_{\rm LC}\eta_{\rm LC}$$
$$=b_{re}\frac{\sigma_e^oN_{\rm LC}\eta_{\rm LC}}{[U_{oe}-E_e(L)]^{1/2}L^4}. \tag{6}$$

Assuming that the LCs are positively charged before illumination, the electron can be captured by the positively charged LC with a very large capture cross-section σ_e^+, then the LC changes to be neutral, and a hole can be captured by the neutral LC with a medium capture cross-section σ_h^o. We have

$$\frac{1}{\tau_{br}}=\frac{V_e\sigma_e^+V_h\sigma_h^o}{V_e\sigma_e^++V_h\sigma_h^o}N_{\rm LC}\eta_{\rm LC}\approx V_h\sigma_h^oN_{\rm LC}\eta_{\rm LC}$$
$$=b_{rh}\frac{\sigma_h^oN_{\rm LC}\eta_{\rm LC}}{(U_{oh}-E_h(L))^{1/2}L^4}. \tag{7}$$

In an actual nanoscale Si/Si oxide system, the sizes of NSPs are not uniform and have a distribution, normally the Gaussian one:

$$\rho(L)=\frac{1}{\sigma\sqrt{2\pi}}\exp\left[-\frac{(L-L_m)^2}{2\sigma^2}\right], \tag{8}$$

where L_m is the most probable size of NSPs, σ the root-mean-square deviation. Assuming further that the sizes for the NSPs have a low limit, which is denoted by L_0, we have

$$\left\langle\frac{1}{\tau_{ar}}\right\rangle=\int_{L_0}^{\infty}\frac{1}{\tau_{ar}}\rho(L)dL \tag{9}$$

and

$$\left\langle\frac{1}{\tau_{br}}\right\rangle=\int_{L_0}^{\infty}\frac{1}{\tau_{br}}\rho(L)dL, \tag{10}$$

where $\langle 1/\tau_{ar}\rangle$ and $\langle 1/\tau_{br}\rangle$ are the average values of $1/\tau_{ar}$ and $1/\tau_{br}$ over the nanoscale Si/Si oxide system, respectively. In Eqs. (9) and (10), the size distribution $\rho(L)$ is given by Eq. (8). Comparing $\langle 1/\tau_{ar}\rangle$ with $\langle 1/\tau_{br}\rangle$, we can see whether the process (A) or (B) is the major one.

For a nanoscale Si/Si oxide system, we can define a critical $N_{\rm LC}$, $N_{\rm LC}^{\rm crit}$, as follows: when $N_{\rm LC}>N_{\rm LC}^{\rm crit}$, we have $\langle 1/\tau_{br}\rangle>\langle 1/\tau_{ar}\rangle$, and when $N_{\rm LC}<N_{\rm LC}^{\rm crit}$, we have $\langle 1/\tau_{ar}\rangle>\langle 1/\tau_{br}\rangle$. $N_{\rm LC}^{\rm crit}$ as a function of L_m can be derived from the following equation:

$$\left\langle\frac{1}{\tau_{ar}}\right\rangle=\left\langle\frac{1}{\tau_{br}}\right\rangle. \tag{11}$$

From Eqs. (1)–(11), $N_{\rm LC}^{\rm crit}$ can be obtained. When the LCs are neutral and $\sigma_e^o\gg\sigma_h^o$, or when the LCs are negatively charged before illumination,

$$N_{\rm LC}^{\rm crit}=\frac{a_r}{b_{re}\eta_{\rm LC}\sigma_e^o}\times\frac{\int_{L_0}^{\infty}\frac{E_0(L)\sin^2(k_0L/2)}{[k_0^2-(2\pi/L)^2]^2L^6}\exp\left[-\frac{(L-L_m)^2}{2\sigma^2}\right]dL}{\int_{L_0}^{\infty}\frac{1}{(U_{0e}-E_e(L))^{1/2}L^4}\exp\left[-\frac{(L-L_m)^2}{2\sigma^2}\right]dL}. \tag{12}$$

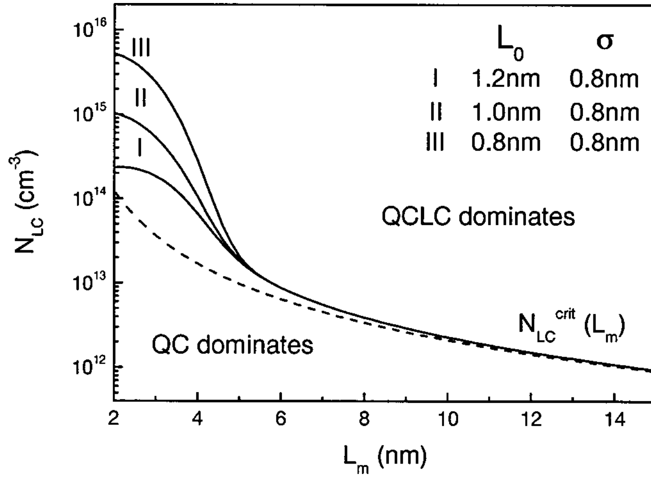

FIG. 2. The $N_{\mathrm{LC}}^{\mathrm{crit}}-L_m$ curves obtained from Eq. (12) with $\sigma=0.8$ nm and $L_0=1.2$, 1.0, and 0.8 nm (solid lines I, II, and III) and from Eq. (16) (dashed line).

When LCs are neutral and $\sigma_h^o \gg \sigma_e^o$, or when the LCs are positively charged the subscripts "e" in Eq. (12) should be substituted by "h".

In Refs. 15–17, the capture cross-sections with the orders of magnitude of 1×10^{-15} cm^2 for some neutral defects and impurities in SiO_2 have been reported. In our numerical calculations we took $\sigma_e^o=1\times10^{-15}$ cm^2, $|P_{cv}|^2/2m=4$ eV and $\eta_{\mathrm{LC}}=10\%$ (as we know porous Si can have a PL efficiency of $\sim$10%). When σ and L_0 for the NSP size distribution of a nanoscale Si/Si oxide system are given, $N_{\mathrm{LC}}^{\mathrm{crit}}$ as a function of L_m can be obtained using Eq. (12). We performed the numerical calculations in the following two cases: (1) suppose $\sigma=0.8$ nm and $L_0=1.2$, 1.0, and 0.8 nm, $N_{\mathrm{LC}}^{\mathrm{crit}}$ as functions of L_m are shown as three solid lines I, II, and III, respectively, in Fig. 2; and (2) suppose $L_0=1.0$ nm and $\sigma=0.8$ and 1.2 nm, $N_{\mathrm{LC}}^{\mathrm{crit}}$ as functions of L_m are shown as two solid lines I and II, respectively, in Fig. 3.

In order to easily compare $\langle 1/\tau_{br}\rangle$ with $\langle 1/\tau_{ar}\rangle$, we get their analytical expressions under the following two further approximations. First, the term $\sin^2(k_oL/2)$ in Eq. (1) is a fast vibrational function of L with a period of $a/0.85=0.64$ nm. While for a nanoscale Si/Si oxide system, the full width of half maximum for NSP size distributions are of $2(2\ln 2)^{1/2}\sigma=2.35\sigma$, which is usually evidently larger than 0.64 nm. Therefore, instead of $\sin^2(k_oL/2)$, its average value of 1/2 can be used approximately. Second, the L in Eqs. (1) and (2) is substituted by its most probable value L_m. Then, we have the Eqs. (13) and (14):

$$\left\langle \frac{1}{\tau_{ar}} \right\rangle \approx \frac{a_r E_0(L_m)}{2[k_0^2-(2\pi/L_m)^2]^2 L_m^6}. \tag{13}$$

When the LCs are neutral and $\sigma_e^o \gg \sigma_h^o$, or when the LCs are negatively charged before illumination:

$$\left\langle \frac{1}{\tau_{br}} \right\rangle \approx \frac{b_{re}\sigma_e^o N_{\mathrm{LC}}\eta_{\mathrm{LC}}}{(U_{0e}-E_e(L_m))^{1/2}L_m^4}. \tag{14}$$

When the LCs are neutral and $\sigma_h^o \gg \sigma_e^o$, or when the LCs are positively charged before illumination, the subscripts "e" in Eq. (14) should be substituted by "h".

When L_m decreases, both $\langle 1/\tau_{ar}\rangle$ and $\langle 1/\tau_{br}\rangle$ increase very fast. $\langle 1/\tau_{ar}\rangle$ increases approximately as L_m^{-6} from Eq. (13), while $\langle 1/\tau_{br}\rangle$ increases approximately as L_m^{-4} from Eq. (14). As shown in Eq. (14), σ_e^o (or σ_h^o), N_{LC} and η_{LC} are important parameters besides L_m for $\langle 1/\tau_{br}\rangle$. We have approximately

$$\frac{\langle 1/\tau_{br}\rangle}{\langle 1/\tau_{ar}\rangle} \propto \sigma^o N_{\mathrm{LC}}\eta_{\mathrm{LC}} L_m^2, \tag{15}$$

where $\sigma^o=\sigma_e^o$, when the LCs are neutral and $\sigma_e^o \gg \sigma_h^o$, or when the LCs are negatively charged before illumination, and $\sigma^o=\sigma_h^o$, when the LCs are neutral and $\sigma_h^o \gg \sigma_e^o$, or when the LCs are positively charged before illumination.

From Eqs. (11), (13) and (14) when the LCs are neutral and $\sigma_e^o \gg \sigma_h^o$, or when the LCs are negatively charged before illumination, we have

$$N_{\mathrm{LC}}^{\mathrm{crit}} \approx \frac{a_r E_0(L_m)(U_{0e}-E_e(L_m))^{1/2}}{2b_{re}\sigma_e^o \eta_{\mathrm{LC}}[k_0^2-(2\pi/L_m)^2]^2 L_m^2}. \tag{16}$$

When the LCs are neutral and $\sigma_h^o \gg \sigma_e^o$, or when the LCs are positively charged before illumination, the subscripts "e" in Eq. (16) should be substituted by "h". The $N_{\mathrm{LC}}^{\mathrm{crit}}$ as an analytical function of L_m obtained from Eq. (16) is depicted by a dashed line in Fig. 2 for case (1) and a dashed line in Fig. 3 for case (2).

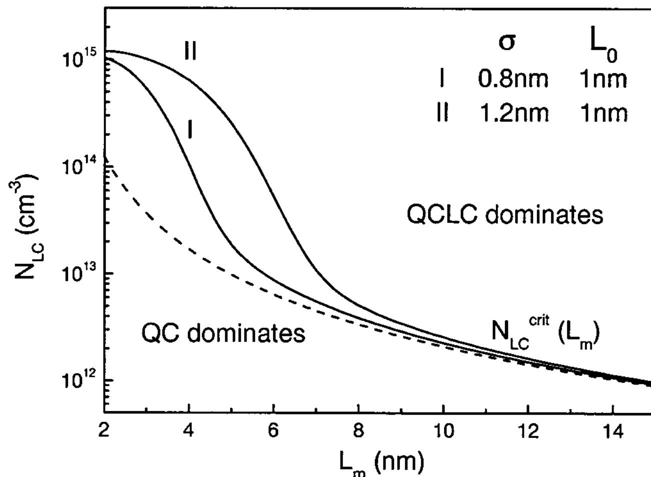

FIG. 3. The $N_{\mathrm{LC}}^{\mathrm{crit}}-L_m$ curves obtained from Eq. (12) with $L_0=1.0$ nm and $\sigma=0.8$ and 1.2 nm (solid lines I and II) and from Eq. (16) (dashed line).

DISCUSSION

For a nanoscale Si/Si oxide system with the (N_{LC}, L_m) points just on the $N_{\mathrm{LC}}^{\mathrm{crit}}-L_m$ curve, such as the one in Fig. 2 or 3, we have $\langle 1/\tau_{ar}\rangle=\langle 1/\tau_{br}\rangle$, which indicates that the QC and QCLC processes have the same rate. For a nanoscale Si/Si oxide systems with the (N_{LC}, L_m) points at the left-down side of the $N_{\mathrm{LC}}^{\mathrm{crit}}-L_m$ curve, we have $\langle 1/\tau_{ar}\rangle > \langle 1/\tau_{br}\rangle$, i.e., the QC process surpasses the QCLC process,

and for a nanoscale Si/Si oxide system with the (N_{LC}, L_m) points at the right-up side of the $N_{\mathrm{LC}}^{\mathrm{crit}}-L_m$ curve, we have $\langle 1/\tau_{br}\rangle > \langle 1/\tau_{ar}\rangle$, i.e., the QCLC process surpasses the QC process. If the (N_{LC}, L_m) points are near the $N_{\mathrm{LC}}^{\mathrm{crit}}-L_m$ curve, both the QC and QCLC processes have to be considered; and if the (N_{LC}, L_m) points are far from the $N_{\mathrm{LC}}^{\mathrm{crit}}-L_m$ curve, only the major one in the QC and QCLC processes should be considered.

From Eq. (15), for a nanoscale Si/Si oxide system, the larger the LC parameters, σ^o, η_{LC}, and N_{LC}, and the larger the NSP most probable size, L_m, the more favorable for the QCLC process to surpass the QC process, and vice versa. With a specific type of LC in SiO_2, the values of η_{LC} and σ^o are fixed. Then N_{LC} and L_m are the two active parameters which determine whether the QC or QCLC process plays the major role in PL. The larger the sizes of NSPs and the higher the density of LCs in SiO_2, the more favorable for the QCLC process than the QC process to occur, and vice versa.

For a nanoscale Si/Si oxide system with $\sigma=0.8$ nm and $L_0=1.0$ nm from Fig. 2, when $L_m=2$, 2.5, 3, 4, 5, and 6 nm, correspondingly, $N_{\mathrm{LC}}^{\mathrm{crit}}=1.0\times10^{15}$, 8.0×10^{14}, 5.3×10^{14}, 1.0×10^{14}, 1.9×10^{13}, and 8.8×10^{12} cm^{-3}, respectively. For most oxidized porous Si and NSP-embedded Si oxide, the NSP size distribution has $L_m>2.5$ nm.[18] Therefore, if $N_{\mathrm{LC}}>8\times10^{14}$ cm^{-3}, the QCLC process dominates the PL. In fact, $N_{\mathrm{LC}}=8\times10^{14}$ cm^{-3} is such a small LC density that there is only one LC in 3×10^{7} SiO_2 molecules in average. Assuming that in the oxidized porous Si, the SiO_2 layers covering the NSPs have a thickness of around 1 nm. When $N_{\mathrm{LC}}=8\times10^{14}$ cm^{-3}, the corresponding Si/SiO_2 interface density is around 8×10^{7} cm^{-2}. If the actual density of the LC at the Si/SiO_2 interface is larger than such a small interface density, the QCLC process dominates the PL. It indicates that if the values of σ^o and η_{LC} for the LCs and the values of L_0 and σ for the NSPs taken in our calculations are proper in the orders of magnitude, for most nanoscale Si/Si oxide systems the QCLC process dominates the PL.

For a nanoscale Si/Si oxide system with definite N_{LC}, we can define a critical L_m, L_m^{crit}, as follows: when $L_m>L_m^{\mathrm{crit}}$, we have $\langle 1/\tau_{br}\rangle > \langle 1/\tau_{ar}\rangle$, i.e., photoemission occurs mainly in the LCs in the Si oxide and when $L_m<L_m^{\mathrm{crit}}$, we have $\langle 1/\tau_{ar}\rangle > \langle 1/\tau_{br}\rangle$, i.e., photoemission occurs mainly inside the NSPs. L_m^{crit} as a function of N_{LC} can be also obtained from Eq. (11), or from the $N_{\mathrm{LC}}^{\mathrm{crit}}-L_m$ curves in Fig. 2 or 3 using the following method: drawing a horizontal line corresponding to the given N_{LC} to get an intersection point on the $N_{\mathrm{LC}}^{\mathrm{crit}}-L_m$ curve, the abscissa of the intersection point is the L_m^{crit} corresponding to the given N_{LC}. For $\sigma=0.8$ nm and $L_0=1.0$ nm, from Fig. 2, when $N_{\mathrm{LC}}=10^{13}$, 10^{14}, and 10^{15} cm^{-3} the corresponding $L_m^{\mathrm{crit}}\approx5.6$, 4.0, and 2.0 nm, respectively. For example, for a nanoscale Si/Si oxide systems with $N_{\mathrm{LC}}=10^{15}$ cm^{-3} we have $L_m^{\mathrm{crit}}=2.0$ nm. It means that for this system when $L_m>2.0$ nm, the QCLC process plays the major role in PL; for $L_m<2.0$ nm, the QC process plays the major role in PL. Since few nanoscale Si/Si oxide systems can have $L_m<2.0$ nm, we conclude again that for most nanoscale Si/Si oxide systems the QCLC process dominates the PL. In general, for NSPs with larger sizes, the QCLC process dominates, while for NSPs with smaller sizes the QC process dominates. This conclusion seems to contradict that of Ref. 10, as already pointed out in the introduction.

All the above conclusions are obtained under several approximations, e.g., the effective mass approximation, infinitely deep well approximation, and the approximate distribution described by Eq. (8) with a lower-limit-size of L_0, etc.. Moreover, when L decreases to very small values, some parameters in the equations such as k_o, m_l, m_t and m_h, might also be functions of L. However, we believed that most qualitative conclusions mentioned above, e.g., the conclusion that "for a nanoscale Si/Si oxide system, the larger the LC parameters, σ^o, η_{LC} and N_{LC} and the larger the NSP most probable size, L_m, the more beneficial for the the QCLC process to surpass the QC process, and vice versa" are still valid qualitatively.

We discuss a couple of experiment results for PL from the nanoscale Si/Si oxide systems using the physical model suggested. It was reported that PL peak energies in a range of 1.4–2.0 eV for more than one hundred as-prepared porous Si samples shifted into a small range centered at 1.70 eV after aging in air for one year or 200 °C oxidation for 200 h.[19] References 20 and 21 independently obtained similar results. Reference 22 reported that PL peak positions for porous Si samples shifted to about 1.69 eV after ozone oxidation. Although preparation conditions and oxidation treatments for porous Si samples in the four papers were quite different, the experimental results were consistent with each other. These experimental results are very difficult to be explained by the QC model, because NSPs will shrink after oxidation and the PL spectra from the porous Si samples should blueshift consistently according to the QC model. However, the result can be explained as follows: after oxidation, suppose that one or several types of LC with luminescence energy near 1.7 eV in Si oxide play the major role in PL, and at least one of these types of LC having a large enough density and/or the sizes of NSPs are large enough so that $\langle 1/\tau_{br}\rangle$ is markedly larger than $\langle 1/\tau_{ar}\rangle$, i.e., the QCLC process through the LCs with the luminescence energy near 1.7 eV in Si oxide markedly surpasses the QC process, therefore, the PL peak energies of oxidized porous Si samples shifted into a small range centered at about 1.7 eV.

Measuring the PL peak energy as a function of the sizes of the NSPs is an important experiment method to check the PL mechanism model. If the PL peak energy shifting with the NSP sizes just consists with what the QC effect predicts, the QC model is verified. If the PL peak energy pins nearly at a fixed energy independent of the sizes of the NSPs, the QCLC model is verified. In fact, the experimental results for how the PL peak energy shifts with the NSP sizes reported by different research groups seemed to contradict each other. Shimizu-Iwayama *et al.* studied the annealing time dependence of the PL spectrum from the NSP-embedded Si oxide obtained by Si-ion implanting into an amorphous SiO_2 matrix.[23] They found the PL peak energy for the implanted Si oxide film was almost independent of the annealing time and thus was independent of the sizes of the NSPs, because their

previous experimental results of cross-section high resolution transmission electron microscopy did verify the growth in sizes of NSPs after increasing the annealing time.[24] However, in the experiment of Brongersma *et al.* the Si nanocrystals (with diameters of 2–5 nm) were formed by Si^+ implantation into a 100-nm-thick thermally grown SiO_2 film on Si(100).[25] The PL spectrum for the NSP-embedded Si oxide peaked at 880 nm which was attributed to the recombination of quantum confined excitons. Upon oxidation at 1100 °C for 30 min the PL peak blueshifted by more than 200 nm. This blueshift was attributed to the QC effect in which a reduction of the average nanocrystal size led to the emission at shorter wavelengths. The apparent contradiction between the experimental result of Shimizu-Iwayama *et al.* and that of Brongersma *et al.* can be explained tentatively as follows: in Shimizu-Iwayama's case the sizes of NSPs and/or the density of LCs in Si oxide were large enough so that the QCLC process dominated the PL, and, therefore, the PL peak energy was almost independent of the sizes of the NSPs. However, in Brongersma's case, the sizes of NSPs and/or the density of LCs were not large enough so that the QC process played an important role in the PL, and thus the PL peak energy evidently depended on the sizes of the NSPs. However, only when the blueshifting is consistent quantitatively with what the QC model predicts, which was discussed recently by Delerue *et al.*,[26] it can be concluded that the QC process plays a decisive role in the PL. Because Ref. 24 did not give the size distributions of the NSPs neither before nor after the annealing, whether or not the blueshifting is consistent with what the QC model predicts cannot be quantitatively discussed.

Rebohle *et al.* presented a review paper on PL and electroluminescence of Si oxide layers ion-implanted with group-IV elements.[27] They found the electroluminescence spectrum correlated very well with the PL one. In the summary of this paper, they stated that "strong PL in the blue-violet spectral region for Si-, Ge-, and Sn-implanted SiO_2 layers is observed which is caused by a molecule-like luminescence center characterized by well defined excitation and emission energies. ... Quantum confinement effects in nanoclusters as a possible origin of this PL can be definitely excluded." We consider the reason for excluding the QC process in NSPs as a major process in PL is that in the Si oxide layers ion-implanted with group-IV elements the LC density is usually large even after annealing and the sizes of the NSPs are typically larger than 3 nm; hence, the rate of the QCLC process normally goes far beyond that of the QC process in these materials. Moreover, the conclusion of Ref. 27 is contrary to that of Ref. 10, which claimed for a nanoscale Si/Si oxide system with the average size of the NSPs larger than or about 3 nm the PL process should take place inside the NSPs. We agree with the conclusion of Ref. 27, however, if the ion-implantation and annealing processes can be excellently controlled to make the LC density in Si oxide low enough and/or the NSP sizes small enough, the QC process may play an important role in PL.

Pavesi *et al.*[28] experimentally proved that the PL process in a nanoscale Si/Si oxide system with an average size of the NSPs of about 3 nm took place at the interface between the Si nanocrystal and the SiO_2 matrix rather than in the NSPs. Their results also seemed to contradict that of Ref. 10.

CONCLUSION

Two competitive photoexcitation-photoemission processes occur in the PL of the nanoscale Si/Si oxide systems, including the oxidized porous Si and the NSP-embedded Si oxide. In the QC process, both photoexcitation and photoemission occur in NSPs, and in the QCLC process, photoexcitation occurs in the NSPs, while the photoemission occurs in the LCs in a Si oxide adjacent to the NSPs. Which process plays the major role in PL is mainly determined by two factors: the sizes of the NSPs and the main parameters of the LC in the Si oxide, which are the capture cross sections of the LC when it is neutral, and the density and luminescence efficiency of the LC. For a nanoscale Si/Si oxide system with a specific type of LC of definite density, a critical most probable size of NSPs can be defined. When the most probable size of the NSPs is larger than the critical one, the QCLC process surpasses the QC process, while when the most probable size of the NSPs is smaller than the critical one, the QC process surpasses the the QCLC process. This conclusion seems contradict to that of Ref. 10. They claimed that for NSPs with larger sizes, the QC model worked, but for NSPs with smaller sizes Si═O bond (a type of LCs) played the key role in light emission. Provided that the key parameters for a nanoscale Si/Si oxide system are given, a $N_{LC}-L_m$ curve can be calculated. For the nanoscale Si/Si oxide systems with the (N_{LC}, L_m) points just on the curve, the QCLC process and the QC process are equal in rate. For a system with the (N_{LC}, L_m) point at the left-down side of the curve, the QC process dominates, and for a system with the (N_{LC}, L_m) point at the right-up side of the curve, the QCLC process dominates. For a system with the (N_{LC}, L_m) point close to the curve, both the QCLC and the QC processes should be taken into account.

ACKNOWLEDGMENT

This work was supported by the National Natural Science Foundation of China.

[1] L. T. Canham, Appl. Phys. Lett. **57**, 1146 (1990).
[2] H. Takagi, H. Ogawa, Y. Yamazaki, A. Ishizaki, and T. Nakagiri, Appl. Phys. Lett. **56**, 2379 (1990).
[3] *Properties of Porous Silicon,* edited by L. Canham (Inspect, London, 1997).
[4] A. Grosman, C. Ortega, J. Siejka, and M. Chamarro, J. Appl. Phys. **74**, 1992 (1993).
[5] G. G. Qin and Y. Q. Jia, Solid State Commun. **86**, 559 (1993).

[6] A. G. Cullis, L. T. Canham and P. D. J. Calcott, J. Appl. Phys. **82**, 909 (1997).
[7] G. G. Qin, J. Lin, J. Q. Duan, and G. Q. Yao, Appl. Phys. Lett. **69**, 1689 (1996).
[8] G. G. Qin, X. S. Liu, S. Y. Ma, J. Lin, G. Q. Yao, X. Y. Lin, and K. X. Lin, Phys. Rev. B **55**, 12 876 (1997).
[9] G. G. Qin, Mater. Res. Bull. **33**, 1857 (1998).
[10] M. V. Wolkin, J. Jorne, P. M. Fauchet, G. Allan, and C. Delerue, Phys. Rev. Lett. **82**, 197 (1999).
[11] M. S. Hybertsen, in *Electronic Structure and Optical Properties of Semiconductors*, edited by M. L. Cohen and J. R. Chelikowsky (Springer-Verlag, New York, 1988).
[12] G. Qin and G. G. Qin, J. Appl. Phys. **82**, 2572 (1997).
[13] G. G. Qin and G. Qin, Phys. Status Solidi A **182**, 335 (2000).
[14] D. L. Dexter, in *Solid State Physics*, edited by F. Seitz and D. Turnbull (Academic, New York, 1958), Vol. 6.
[15] T. H. Ning, J. Appl. Phys. **49**, 4077 (1978).
[16] X. Gao and S. S. Yee, Solid-State Electron. **39**, 399 (1996).
[17] A. Palma, J. A. Lopez-Villanueva and J. E. Carceller, J. Electrochem. Soc. **143**, 2687 (1996).
[18] For examples: K. Ito, S. Ohyama, Y. Uehara, and S. Ushioda, Appl. Phys. Lett. **67**, 2536 (1995); M. Binder, T. Edelmann, T. H. Metzger, G. Mauckner, G. Goerigk, and J. Peisl, Thin Solid Films **276**, 65 (1996); L. P. You, C. L. Heng, S. Y. Ma, Z. C. Ma, W. H. Zong, Z. L. Wu, and G. G. Qin, J. Cryst. Growth **212**, 109 (2000).
[19] G. G. Qin, H. Z. Song, B. R. Zhang, J. Lin, J. Q. Duan, and G. Q. Yao, Phys. Rev. B **54**, 2548 (1996).
[20] I. M. Chang and Y. F. Chen, J. Appl. Phys. **82**, 3514 (1997).
[21] J. Harper and M. J. Sailor, Langmuir **13**, 4652 (1997).
[22] L. Jia, S. P. Wang, I. H. Wilson, S. K. Hark, S. L. Zhang, Z. F. Liu, and S. M. Cai, Appl. Phys. Lett. **71**, 1391 (1997).
[23] T. S. Iwayama, N. Kurumado, D. E. Hole, and P. D. Townsend, J. Appl. Phys. **83**, 6018 (1998).
[24] T. S. Iwayama, Y. Terao, A. Kamiya, M. Takeda, S. Nakao, and K. Saitoh, Nanostruct. Mater. **5**, 307 (1995).
[25] M. L. Brongersma, A. Polman, K. S. Min, E. Boer, T. Tambo, and H. A. Atwater, Appl. Phys. Lett. **72**, 2577 (1998).
[26] C. Delerue, M. Lannoo, and G. Allan, in *Properties of Porous Silicon* (Ref. 3), p. 212.
[27] L. Rebohle, J. von Borany, H. Frob and W. Skorupa, Appl. Phys. B: Lasers Opt. **71**, 131 (2000).
[28] L. Pavesi, L. Dal Negro, C. Mazzoleni, G. Franzo, and F. Priolo, Nature (London) **408**, 440 (2000).